



Facile Hydrothermal Procedure for the Synthesis of Sodium Aluminum Silicate Hydrate/Analcime and Analcime for Effective Removal of Manganese(II) Ions From Aqueous Solutions

Hany M. Youssef^{1,2} · Reem K. Shah³ · Faisal K. Algethami⁴ · R. M. Hegazey⁵ · Ahmed M. Naglah^{6,7} · Mohamed A. Al-Omar⁶ · Ahmad A. Alluhaybi⁸ · Hatim A. Alherbish⁹ · E. M. Mabrouk¹⁰ · Ehab A. Abdelrahman¹⁰

Received: 12 July 2020 / Accepted: 31 July 2020 / Published online: 7 August 2020
© Springer Science+Business Media, LLC, part of Springer Nature 2020

Abstract

In this research, sodium aluminum silicate hydrate/analcime composite (abbreviated as S/A) and analcime (abbreviated as A) products were fabricated utilizing the hydrothermal technique in the absence and presence of glutamine (concentration = 0.0435 g/mL) as phase-controlling template, respectively. Glutamine behaves as a crowning agent and avoids the accretion of particles. Hence, it controlled the morphology, aluminum silicate type, and crystallite size. The patterns of XRD elucidated that the S/A composite and A products exhibit a crystallite size equals 70.36 and 80.24 nm, respectively. Besides, the SEM elucidated that the S/A composite comprised of an irregular and sphere forms with a size of 2.64 μm whereas the A product comprised of a droxtal forms with a size of 7.84 μm . Furthermore, the fabricated products were exploited for removing Mn(II) ions from aqueous solutions. The uptake of Mn(II) ions was constrained by the pseudo-second-order model and Langmuir isotherm. Besides, the uptake of Mn(II) ions was exothermic since the estimations of ΔH° on account of S/A composite and A product were -52.059 and -58.878 kJ/mol, respectively. Additionally, the maximum uptake capacity of S/A composite and A product was 75.188 and 60.241 mg/g, respectively. The higher uptake of the S/A composite can be explained by the fact that the S/A composite has a small crystallite size (70.36 nm) and a high surface area (20.26 m^2/g) compared to the A product. Furthermore, the fabricated products are returnable, stable, effective, and can be reutilized more than once without the concession of their efficacy regarding Mn(II) ions.

Keywords Aqueous media · Sodium aluminum silicate hydrate/analcime composite · Analcime · Manganese(II) ions · Removal parameters

✉ Hany M. Youssef
hanyyoussef178@gmail.com

¹ Department of Chemistry, College of Science and Humanities in Al-Kharj, Prince Sattam Bin Abdulaziz University, Al-Kharj 11942, Saudi Arabia

² Department of Chemistry, Faculty of Science, Mansoura University, Mansoura 35516, Egypt

³ Department of Chemistry, Faculty of Applied Science, Umm Al-Qura University, Makkah 21955, Saudi Arabia

⁴ Department of Chemistry, Faculty of Science, Imam Mohammad Ibn Saud Islamic University, Riyadh, Saudi Arabia

⁵ Egyptian Petroleum Research Institute, Ahmed El Zumer Street, Nasr City, Hai Al-Zehour, Cairo 11727, Egypt

⁶ Drug Exploration & Development Chair (DEDC), Department of Pharmaceutical Chemistry, College of Pharmacy, King Saud University, Riyadh 11451, Saudi Arabia

⁷ Peptide Chemistry Department, Chemical Industries Research Division, National Research Centre, Dokki, Cairo 12622, Egypt

⁸ Department of Chemistry, Rabigh College of Science and Arts, King Abdulaziz University, Rabigh 21911, Saudi Arabia

⁹ Saudi Food and Drug Authority, Research and Laboratory Sector, Department of Food Laboratory, Riyadh, Saudi Arabia

¹⁰ Chemistry Department, Faculty of Science, Benha University, Benha 13518, Egypt

1 Introduction

It has notable that the intensification of pollutants in water resources via different human and industrial performances can make difficult problems for plants, humans, and animals. The significant gatherings of environmental contamination are heavy metals and organic molecules [1–6]. The elevated concentration of heavy metal ions, especially Mn(II) ions, in drinking water above the permissible level (50 µg/L) leads to several neurological deformities, for example, Parkinson's disease according to the World Health Organization (WHO) rules [7, 8]. Manganese causes many health troubles such as hallucinations, forgetfulness, nerve decay, bronchitis, and heart or valves tissue irritation. Owing to the altering of turbidity, taste, and color of water in the existence of Mn(II) ions and abnormalities referenced previously, fitting methods for the uptake of these ions from aqueous solutions have been established by scientists. Among the treatment approaches for removing toxic ions such as manganese ions, adsorption using an appropriate cost-effective and eco-friendly adsorbent is more applicable than different procedures including chemical precipitation, reverse osmosis, oxidation, ultrafiltration, etc. [9–11]. The elevated adsorption capacity of certain adsorbents such as ferric oxides, alumina, and activated carbon is the main object for their extensive utilization for removing various metals ions from aqueous solutions [12–14]. Such points of interest were restricted by their significant expense. Hence, searching attempts for low-cost and eco-friendly adsorbent materials dominate on these problems. An effective candidate adsorbent for this point is aluminum silicates (i.e. zeolites). Zeolites are considered as wonderful cation exchangers because they possess a net negative charge, which compensated by the exchangeable ions of positive charge such as sodium ions, and consequently elevated adsorption capacity toward different cations such as Zn(II), Cu(II), and Pb(II) ions [15–17]. Removing of inorganic pollutants using clinoptilolite zeolite of natural type concerning Mn(II), Zn(II), Cu(II), and Co(II) were examined by Erdem et al. [18, 19]. The study accomplished utilizing batch procedure and the influence of changing the primary concentration of previous metal ions also examined. They found that the uptake process is occurred according to the following order $\text{Co(II)} > \text{Cu(II)} > \text{Zn(II)} > \text{Mn(II)}$. Also, the removal of Ni(II), Co(II), La(III), and Ba(II) ions from aqueous media was examined by Sofia et al. [20]. The study accomplished utilizing batch technique using platinum/Zeolite-4A adsorbent. They found that the optimum adsorption conditions were achieved at dosage = 0.2 g/20 mL, pH 7, and contact time = 30 min. Besides, the synthesis of various zeolite adsorbents from

fly ash was examined by Min-Gyu et al. [21]. By the utilize of several temperatures and sodium hydroxide concentrations, five zeolites were gotten: faujasite, Na-P1, analcime, cancrinite, and hydroxysodalite. Na-P1 zeolite showed the highest uptake capacity toward Pb ions (1.29 mmol/g). Consequently, due to the high adsorption capacity of zeolite toward a lot of pollutants, many researchers devote their time to find simple and inexpensive synthetic methods. Lately, organic molecules behave as a crowning agent and avoid the accretion of particles. Hence, they controlled the morphology, aluminum silicate type, and crystallite size [17, 22, 23]. In this work, sodium aluminum silicate hydrate/analcime (S/A) composite and analcime (A) products were hydrothermally produced in the absence of template and the presence of glutamine, respectively. Moreover, the efficiency of the fabricated products in the uptake of Mn(II) ions from aqueous media were estimated.

2 Experimental

2.1 Chemicals

Nitric acid (Chemical formula: HNO_3), fumed silica (Chemical formula: SiO_2), sodium hydroxide (Chemical formula: NaOH), aluminum chloride hexahydrate (Chemical formula: $\text{AlCl}_3 \cdot 6\text{H}_2\text{O}$), hydrochloric acid (Chemical formula: HCl), glutamine (Chemical formula: $\text{C}_5\text{H}_{10}\text{N}_2\text{O}_3$), ethylenediaminetetraacetic acid tetrasodium salt dihydrate (EDTA) (Chemical formula: $\text{C}_{10}\text{H}_{16}\text{N}_2\text{Na}_4\text{O}_{10}$), and manganese(II) chloride tetrahydrate (Chemical formula: $\text{MnCl}_2 \cdot 4\text{H}_2\text{O}$) were attained from Sigma Aldrich company.

2.2 Synthesis of Analcime and Sodium Aluminum Silicate Hydrate/Analcime

93 mL of 2.27 mol/L sodium hydroxide was utilized for dissolving 2.87 g of fumed silica for obtaining Si(IV) solution. Besides, 30 mL of distilled water was employed for dissolving 2.87 g of aluminum chloride hexahydrate for obtaining Al(III) solution. Also, 23 mL of 1.27 mol/L sodium hydroxide was employed for dissolving 1 g of glutamine for obtaining template precursor. After that, the glutamine solution was poured to the Si(IV) solution partially wise with continuous stirring for 43 min. Then, the Al(III) solution was poured to the glutamine/Si(IV) mixture partially wise with continuous stirring for 43 min. Furthermore, the resulting glutamine/Al(III)/Si(IV) mixture was exposed to 123 °C till the overall volume matches 83 mL. Then, the glutamine/Si(IV)/Al(III) mixture was transported into Teflon lined autoclave) capacity = 100 mL(then exposed to 123 °C for 1 day. Furthermore, the white precipitate (analcime: abbreviated as A) was filtered, washed several times

using hot distilled water, dried at 83 °C for 1 day, and calcined at 550 °C for 5 h. The previous experimental steps were repeated, but in the absence of the glutamine to obtain sodium aluminum silicate hydrate/analcime composite (abbreviated as S/A).

2.3 Uptake of Manganese Ions From Aqueous Solutions

Uptake batch tries were accomplished via moving a 0.04 g of the A product or S/A composite into a 0.25 L Erlenmeyer conical flask including 35 mL of a particular Mn(II) concentration adjusted to a specific pH consuming 0.1 M HCl or NaOH. Several factors were accomplished such as pH (in the range of 2.5–8 at contact time = 120 min and concentration = 180 mg/L), contact time (in the range of 5–180 min at pH 6 and concentration = 180 mg/L), temperature (in the extent of 298–323 K at contact time = 60 min, pH 6, and concentration = 180 mg/L), and concentration (in the extent of 60–240 mg/L at contact time = 60 min and pH 6). After that, the combines were magnetically mixed via exploiting a magnetic stirrer (speed = 470 rpm). Then, the A product or S/A composite was withdrawn employing a centrifuge (speed = 2503 rpm). Besides, the filtrate was investigated for manganese ions via exploiting inductively coupled plasma (ICP). The quantity of Mn(II) ions taken by unit mass (g) of the A product or S/A composite (Q, mg/g) was estimated through the subsequent expression;

$$Q = (C_i - C_{eq}) V/m \quad (1)$$

Besides, the % uptake of Mn(II) ions using the A product or S/A composite (% R) was estimated through the subsequent expression;

$$\% R = (C_i - C_{eq}) * 100/C_i \quad (2)$$

where, C_{eq} (mg/L) and C_i (mg/L) expressions are the concentration of the Mn(II) ions in the filtrate and primary solution, respectively. Furthermore, V (L) expression is the solution volume. Besides, m (g) expression is the quantity of the S/A composite or A product.

Desorption batch experiments were accomplished via transporting a manganese loaded A product or S/A composite into a 0.25 L conical flask including 35 mL of desorption reagents such as HNO₃ (0.15 and 0.6 M), HCl (0.15 and 0.6 M), and EDTA (0.15 and 0.6 M). After that, the mixes were magnetically mixed via exploiting a magnetic stirrer (speed = 470 rpm) for 50 min at room temperature. Furthermore, the S/A composite or A product was separated via exploiting a centrifuge (speed = 2503 rpm). Besides, the filtrate was investigated for manganese ions via exploiting inductively coupled plasma (ICP).

Also, the desorption fraction (% S) was estimated through the subsequent expression;

$$\% S = (100 C_{dm} V_{dm}) / ((C_i - C_{eq}) V) \quad (3)$$

where, V_{dm} (L) term is the volume of desorption reagent and C_{dm} (mg/L) term is the concentration of Mn(II) ions which exist in the desorption reagent. Furthermore, the separated A product or S/A composite was exposed to 73 °C for drying then reprocessed four periods as formerly illustrated.

2.4 Characterization

The X-ray diffraction patterns (XRD) of the S/A composite or A product were recorded utilizing a D8 Advance Bruker X-ray diffractometer with Cu K α irradiation ($\lambda = 0.15$ nm). Also, Fourier-transform infrared images (FT-IR) of S/A composite or A product were gotten using the Perkin Elmer FT-IR spectrophotometer. The morphology images of the S/A composite or A product were gotten via exploiting scanning electron microscopy (SEM, JEOL, JSM.6510LV). Thermo Scientific 6500 Duo Inductively coupled plasma was employed for the estimation of Mn(II) concentration.

3 Results and Discussion

3.1 Identification of the Fabricated Products

Figure 1a clarifies the XRD pattern of the S/A composite which was constructed in the absence of templates. Also, Fig. 1b clarifies the XRD pattern of the A product which was constructed using glutamine.

The chemical formula, crystal structure, and space group of analcime are Na (AlSi₂O₆) (H₂O), Cubic, and Ia-3d, respectively as simplified in JCPDS No. 70-1575 [16, 24, 25]. Also, the chemical formula, crystal structure, and space group of sodium aluminum silicate hydrate are Na₆ (AlSiO₄)₆.8H₂O, Cubic, and P-43n, respectively as simplified in JCPDS No. 40-0102 [16, 24, 25].

The specific peaks of the analcime zeolite at $2\theta = 68.99, 66.01, 63.11, 57.71, 56.86, 54.23, 53.34, 52.43, 48.69, 47.73, 40.47, 37.01, 35.79, 33.25, 31.91, 30.51, 25.94, 24.24, 18.26, \text{ and } 15.80$ can be ascribed to lattice plans of (772), (932), (921), (831), (660), (741), (800), (732), (633), (640), (532), (440), (521), (431), (422), (332), (400), (321), (220), and (211), respectively. Also, the specific peaks of the sodium aluminum silicate hydrate at $2\theta = 65.02, 61.03, 59.00, 50.48, 43.35, 38.02, 35.13, 24.61, 20.00, \text{ and } 14.11$ can be ascribed to lattice plans of (611), (530), (440), (422), (330), (321), (222), (211), (200), and (110), respectively.

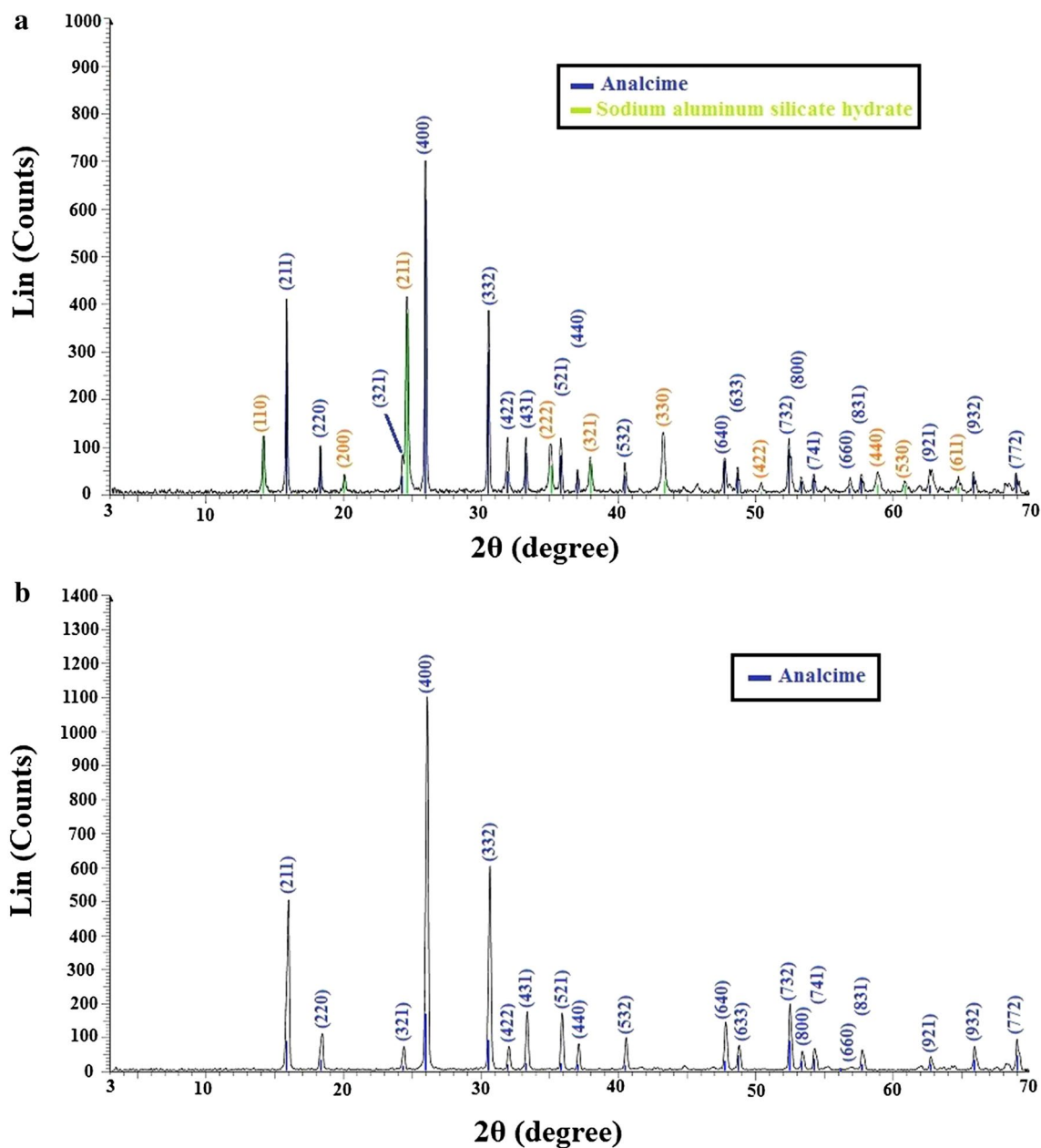


Fig. 1 XRD of the S/A composite (a) and A (b) samples

The A product and S/A composite possess a crystallite size, which was evaluated applying Scherrer equation, equals 80.24 and 70.36 nm, respectively [26–31].

Figure 2a, b clarifies the FT-IR spectra of the S/A composite and A samples, respectively. The broadband, which was observed in S/A composite or A product at 3450/cm, was assigned to the stretching vibration of water (H_2O), silanol (Si–OH), and/or aluminol (Al–OH) functional groups. Also, the noticed bands in S/A composite and A product at 1648 and 1649/cm were ascribed to the bending vibration of zeolite water, respectively. Besides, the

observed bands at 450 and 451/cm in S/A composite and A product were ascribed to the bending vibration of X–O–X (X = Si and/or Al), respectively. Additionally, the noticed band at 589/cm in S/A composite indicated the vibration of a double ring. Further, the noticed band in S/A composite or A product at 672/cm indicated the internal symmetric vibration of X–O–X. Also, the noticed bands in S/A composite (at 712 and 783/cm) and A product (at 785/cm) indicated the external symmetric vibration of X–O–X. Besides, the noticed bands in S/A composite and A product at 1037 and 1031/cm were ascribed to the internal asymmetric vibration

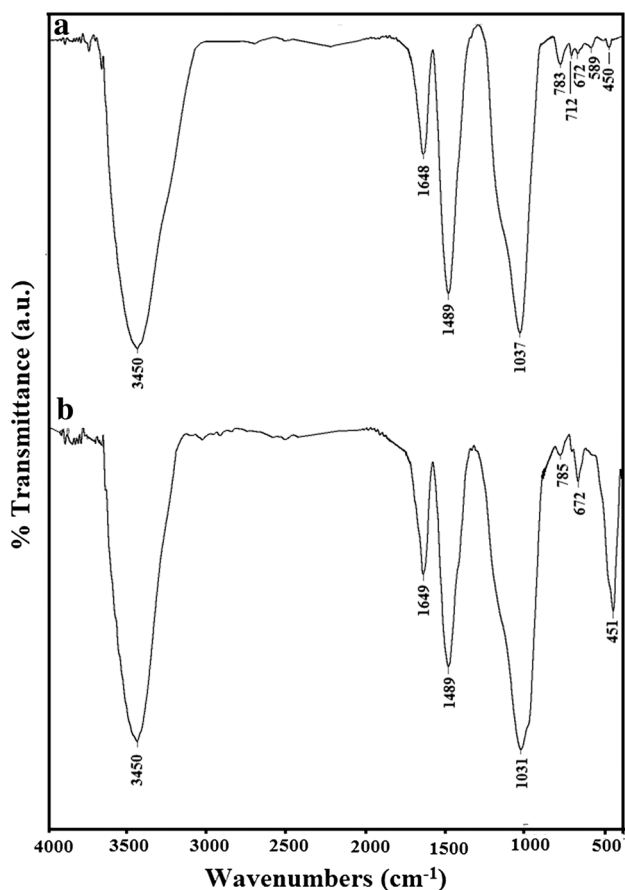


Fig. 2 FT-IR spectra of the S/A composite (a) and A (b) samples

of X-O-X, respectively. Furthermore, the noticed band in S/A composite or A product at 1489/cm was ascribed to the external asymmetric vibration of X-O-X [15–17, 22, 23].

Figure 3a, b clarifies the images of FE-SEM for the S/A composite and A product, respectively. Also, the S/A composite comprised of an irregular and sphere forms with a size equals 2.64 μm . Besides, the A product comprised of droxtal

forms with a size equals 7.84 μm . BET surface area, which was determined from nitrogen isotherms at $-196\text{ }^\circ\text{C}$, for S/A composite and A products equals 20.26 and 13.87 m^2/g , respectively.

3.2 Uptake of Mn(II) Ions From Aqueous Solutions

3.2.1 Impact of Solution pH

The % removal (% R) and uptake capacity (Q), which were tested in the range of pH 2.5–8.0 for S/A composite and A product, were simplified in Fig. 4a, b, respectively. Q or % R quickly rises with the rise in the value of pH for Mn(II) solution then subsequently reached to approximately plateau estimate about 6.50. On account of S/A composite, Q and % R at pH 6.5 were 61.25 mg/g and 38.89%, respectively. Besides, on account of A product, Q and % R at pH 6.5 were 43.75 mg/g and 27.78%, respectively.

3.2.2 Impact of Contact Time

The % removal (% R) and uptake capacity (Q), which were tested in the range of time = 5–180 min for S/A composite and A product, were simplified in Fig. 5a, b, respectively. Q or % R quickly grows with the rise in the time for manganese solution then arrived at approximately plateau estimate at 60 min. On account of S/A composite, Q and % R at time = 60 min were 59.50 mg/g and 37.78%, respectively. Also, on account of A product, Q and % R at time = 60 min were 45.50 mg/g and 28.89%, respectively.

Two essential adsorption kinetic models, pseudo-first-order (Eq. 4) and pseudo-second-order (Eq. 5) were employed for matching the experimental data [15–17, 22, 23, 32, 33].

$$\log(Q_e - Q_t) = \log Q_e - K_F t / 2.303 \quad (4)$$

$$t/Q_t = (1/K_S Q_e^2) + (1/Q_e) t \quad (5)$$

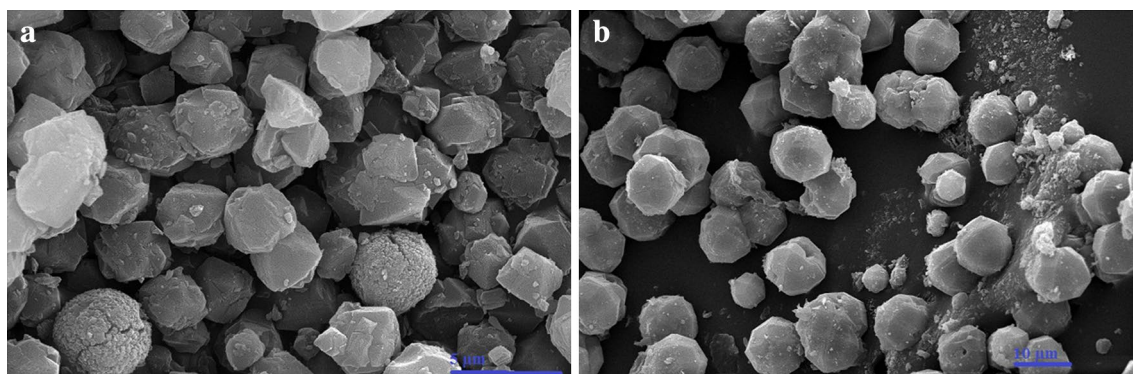


Fig. 3 SEM images of the S/A composite (a) and A (b) samples

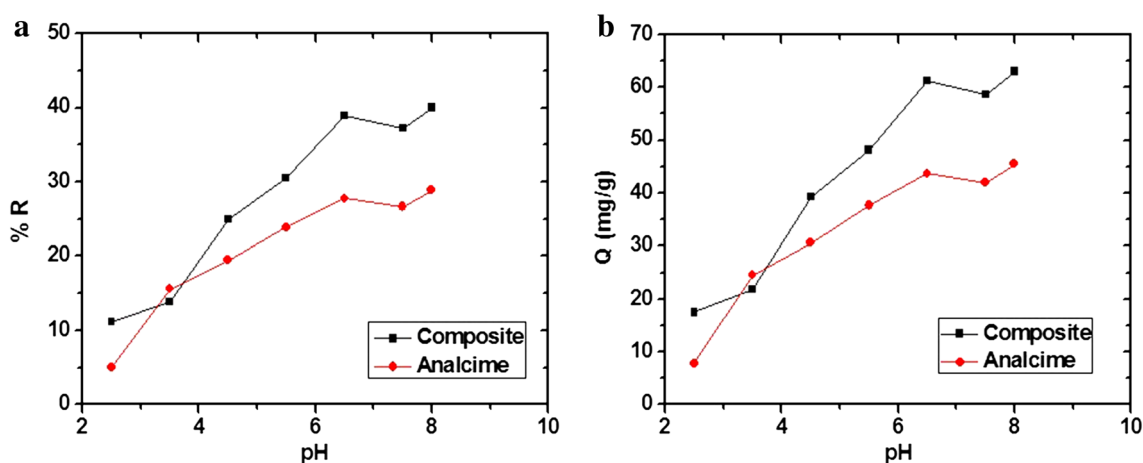


Fig. 4 The relation of pH with % R of manganese ions (a) and uptake capacity of the synthesized samples (b)

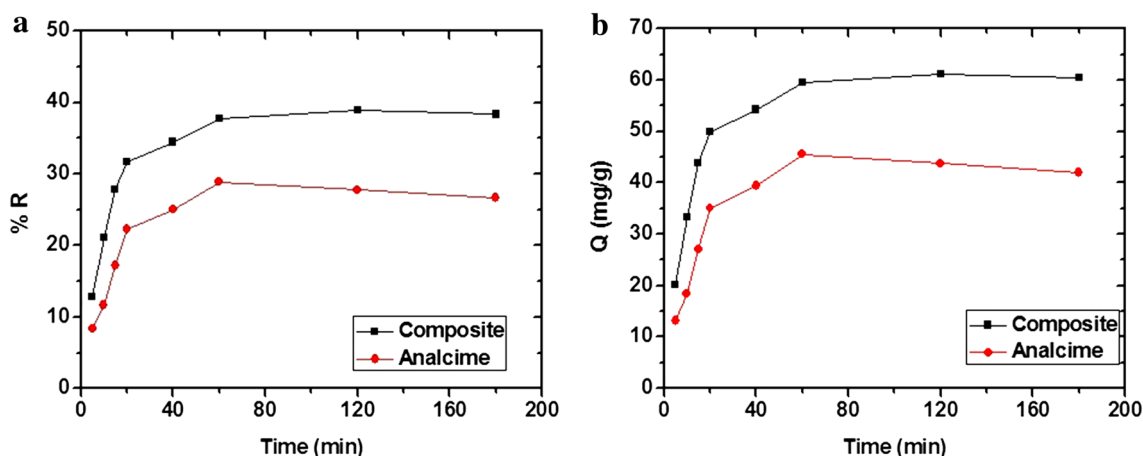


Fig. 5 The relation of time with % R of manganese ions (a) and uptake capacity of the synthesized samples (b)

where, the term of Q_e (mg/g) represents the uptake capacity toward Mn(II) ions at equilibrium whereas the term of Q_t (mg/g) represents the uptake capacity at contact time t . Also, K_F (1/min) expression is the rate constants of pseudo-first-order whereas K_S (g/mg min) expression is the rate constants of pseudo-second-order models. The pseudo-first-order (a linear plot of $\log(Q_e - Q_t)$ vs. t) and pseudo-second-order (a linear plot of t/Q_t vs. t) models on account of utilizing S/A composite or A product were shown and explained exploiting Fig. 6a, b, respectively. The evaluated kinetic factors due to the adsorption of Mn(II) ions using S/A composite or A product were presented in Table 1. Also, the correlation coefficient values (R^2), which were acquired from the pseudo-second-order model on account of S/A composite or A product, were more than that of the pseudo-first-order model. Hence, the adsorption processes of Mn(II) ions were constrained by the pseudo-second-order model.

3.2.3 Impact of Solution Temperature

The % removal (% R) and adsorption capacity (Q), which were examined in the range of temperature = 298–328 K for S/A composite and A product, were presented in Fig. 7a, b, respectively. Adsorption capacity (Q) or % removal (% R) quickly reduces with the rise in the value of temperature for manganese solution.

The ΔH° (change in enthalpy), ΔG° (change in free energy), and ΔS° (change in the entropy) factors due to the uptake of manganese ions were evaluated utilizing equations No. 6 and 7 [15–17, 22, 23, 32, 33].

$$\Delta G^\circ = \Delta H^\circ - T\Delta S^\circ \quad (6)$$

$$\ln K_d = (\Delta S^\circ/R) - (\Delta H^\circ/RT) \quad (7)$$

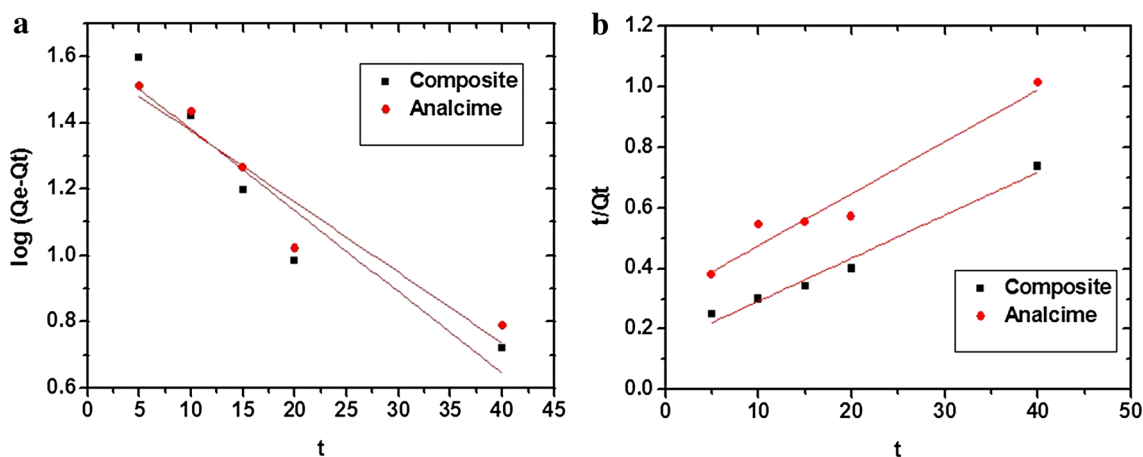


Fig. 6 The pseudo-first-order (a) and pseudo-second-order (b) models

Table 1 The constants of pseudo-first-order and pseudo-second-order models

Adsorbent	Pseudo first order			Pseudo second order		
	Q (mg/g)	K_F (1/min)	R^2	Q (mg/g)	K_S (g/mg min)	R^2
Composite	42.047	0.056	0.882	70.472	0.001	0.976
Analcime	38.569	0.049	0.9	58.275	0.001	0.934

where, the term of K_d (L/g) represents the distribution coefficient whereas T (Kelvin) expression is the uptake temperature. Also, R (KJ/mol K) expression is the value of a gas constant. Furthermore, the distribution coefficient (K_d) was calculated through Eq. (8).

$$K_d = Q/C_{eq} \quad (8)$$

Linear plots of $\ln K_d$ vs. $1/T$ were clarified in Fig. 7c. The calculated thermodynamic constants due to the uptake of Mn(II) ions using A product or S/A composite were displayed in Table 2. The value of ΔH° on account of S/A composite and A product is -52.059 and -58.878 kJ/mol, respectively. So, the uptake of Mn(II) ions utilizing S/A composite and A product is chemical (due to $\Delta H^\circ \geq 40$ kJ/mol) and exothermic (due to the negative sign). The values of ΔG° on account of S/A composite and A product are -105.207 and -119.819 kJ/mol at temperature equals 25°C , respectively. So, the uptake of manganese ions employing A product or S/A composite is spontaneous due to the negative sign. The values of ΔS° on account of S/A composite and A product are 0.178 and 0.205 kJ/molK, respectively. So, the uptake of manganese ions was extremely disordered at the solution boundary/adsorbent due to the positive sign.

3.2.4 Impact of Primary Metal Concentration

The % removal (% R) and uptake capacity (Q), which were tested in the range of concentration = 60–240 mg/L for

S/A composite and A product, were displayed in Fig. 8a, b, respectively. Adsorption capacity (Q) quickly increases whereas % removal (% R) reduces with the rise in the primary concentration of manganese ions. Two essential uptake equilibrium models, Freundlich (Eq. 9) and Langmuir (Eq. 10) were employed for matching the obtained experimental data [15–17, 22, 23, 32, 33].

$$\ln Q_e = \ln K_{Fr} + (1/n) \ln C_e \quad (9)$$

$$C_e/Q_e = (1/K_L Q_m) + (C_e/Q_m) \quad (10)$$

where, Q_m (mg/g) expression is the maximum uptake capacity whereas K_{Fr} (mg/g)(L/mg) $^{1/n}$ expression is the Freundlich constant. Also, K_L (L/mg) expression is the Langmuir constant whereas $1/n$ expression is the heterogeneity factor. Furthermore, the Q_m of Freundlich isotherm was calculated with the aid of Eq. (11).

$$Q_m = K_F(C_i)^{1/n} \quad (11)$$

The Freundlich and Langmuir isotherms on account of employing S/A composite and A product were conducted and explained exploiting Fig. 9a, b, respectively. The calculated equilibrium constants due to the uptake of manganese ions using S/A composite and A product were donated in Table 3. Also, the correlation coefficient values (R^2), which were acquired from the Langmuir isotherm on account of

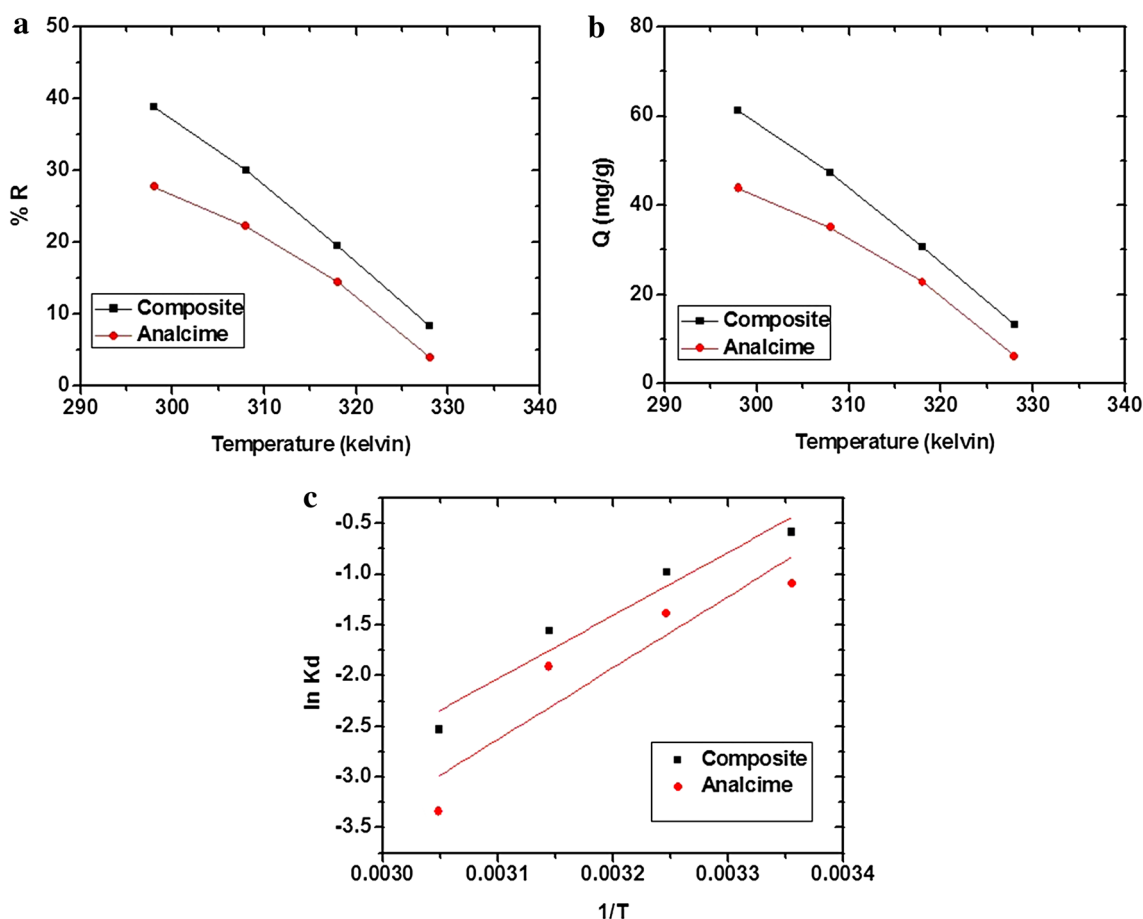


Fig. 7 The relation of temperature with % R of manganese ions (a) and uptake capacity of the synthesized samples (b). The plots of $\ln K_d$ versus $1/T$ (c)

Table 2 The thermodynamic parameters

Adsorbent	ΔG° (KJ/mol)				ΔS° (KJ/molK)	ΔH° (KJ/mol)
	Temperature (Kelvin)					
	298	308	318	328		
Composite	-105.207	-106.991	-108.774	-110.558	0.178	-52.059
Analcime	-119.819	-121.865	-123.909	-125.955	0.205	-58.878

S/A composite and A product, were more than that of the Freundlich isotherm. Hence, the uptake of Mn(II) ions was constrained by the Langmuir isotherm. Furthermore, the maximum uptake capacity of S/A composite and A product was 75.188 and 60.241 mg/g, respectively.

3.2.5 Impact of Regeneration and Reusability

For making the adsorption technique more progressively economical, the regenerations of the utilized adsorbents are important. 0.15 M HNO₃, 0.6 M HNO₃, 0.15 M HCl, 0.6 M HCl, 0.15 M EDTA, and 0.6 M EDTA freshly

prepared solutions were operated for the desorption of manganese ions from S/A composite and A product as shown in Fig. 10a, b, respectively. % S equals 99.29 and 99.04% on account of S/A composite and A product by means of 0.6 M EDTA. So, EDTA was employed for desorption of Mn(II) ions from S/A composite and A product. The reusability of S/A composite and A product for four periods was displayed in Fig. 11a, b, respectively. There is an extremely insignificant reduction in the % uptake of Mn(II) ions applying S/A composite and A product. Hence, the S/A composite or A adsorbents are returnable,

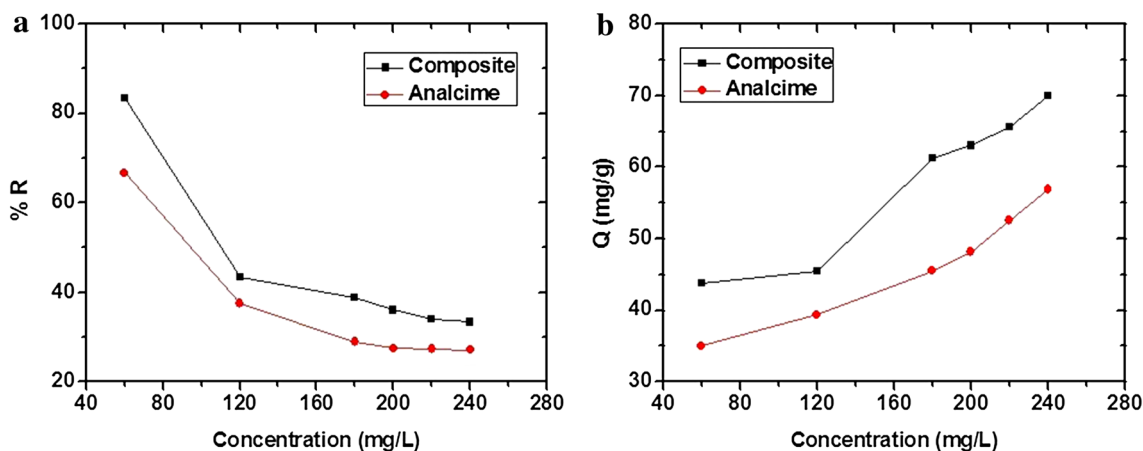


Fig. 8 The relation of concentration with % R of manganese ions (a) and uptake capacity of the synthesized samples (b)

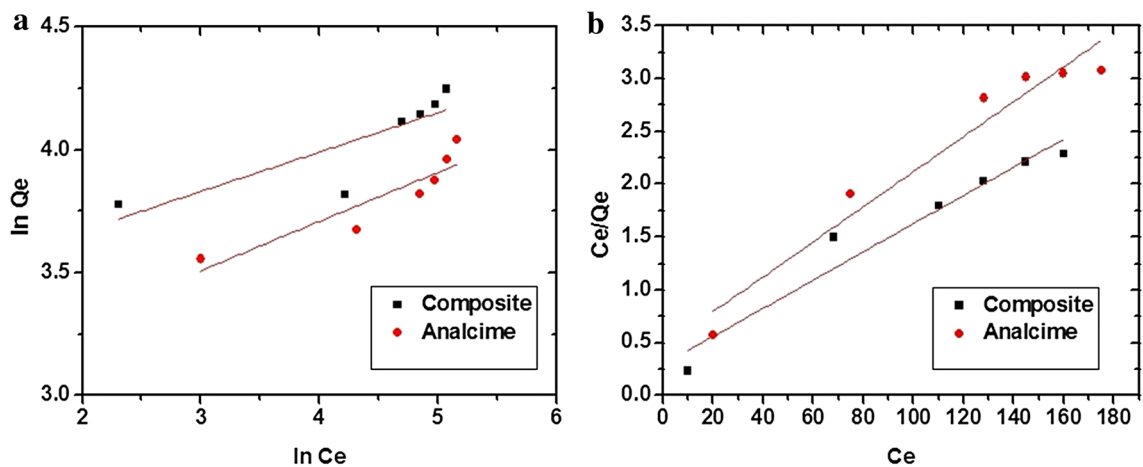


Fig. 9 The Freundlich (a) and Langmuir (b) isotherms

Table 3 The constants of Langmuir and Freundlich isotherms

Adsorbent	Langmuir			Freundlich		
	Q_m (mg/g)	K_L (L/mg)	R^2	Q_m (mg/g)	K_{Fr} (mg/g)(L/mg) ^{1/n}	R^2
Composite	75.188	0.046	0.937	65.527	28.459	0.646
Analcime	60.241	0.036	0.938	51.718	18.353	0.786

stable, effective, and can be used over and over without the concession of their efficacy regarding Mn(II) ions.

3.2.6 Comparative Investigation

The uptake capacity of the S/A composite or A product regarding manganese ions were compared with further adsorbent materials in the previous papers, for example, metakaolin established geopolymer, EDTA-improved magnetic activated carbon nanocomposite, Mo/Co double layered hydroxide,

activated carbon immobilized via tannic acid, and Crab shell as clarified in Table 4 [11, 34–38]. The uptake capacities of the constructed samples toward Mn(II) ions outperform most of the above-mentioned adsorbents.

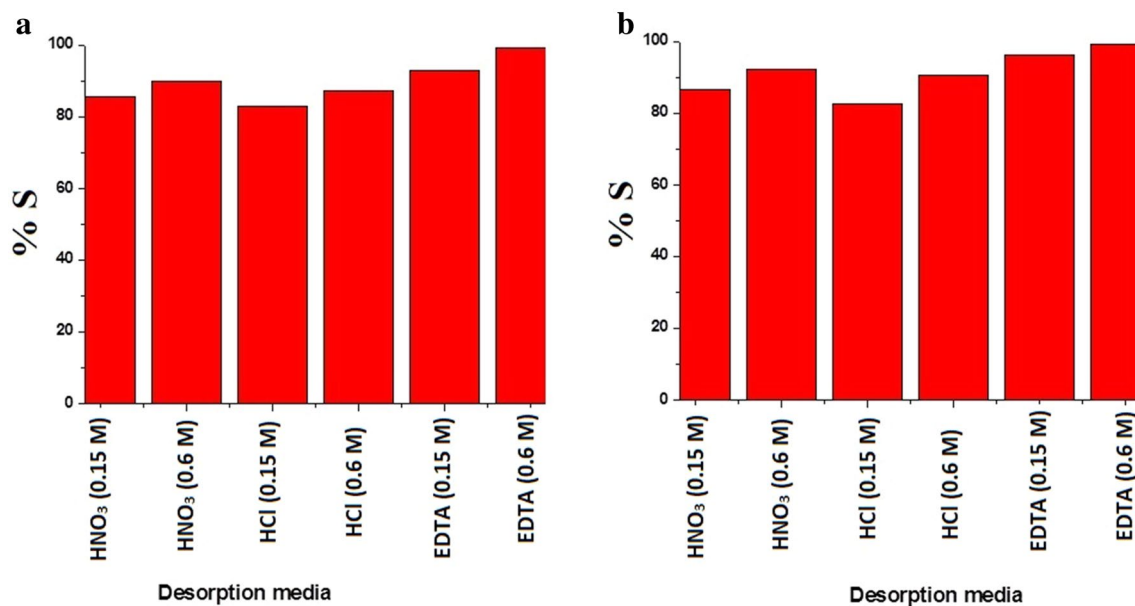


Fig. 10 The relation of % S with desorption media for S/A composite (a) and A (b) samples

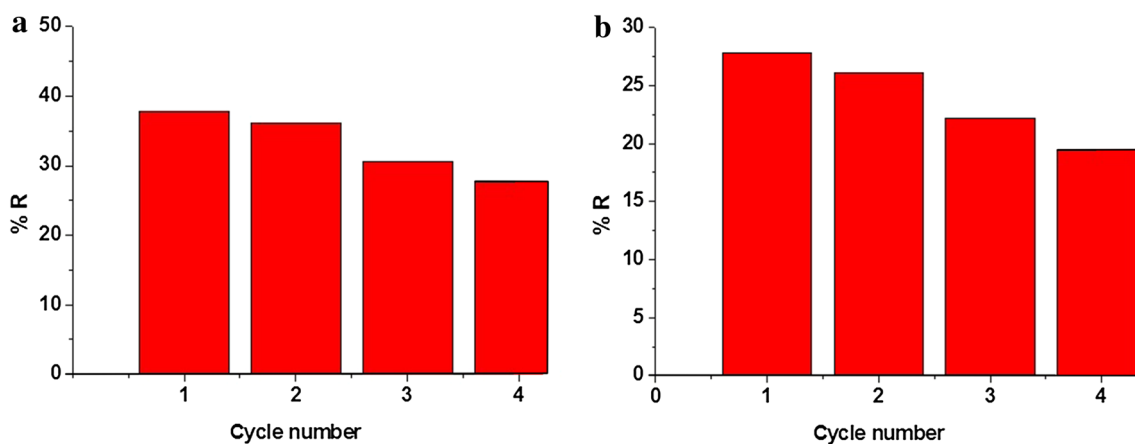


Fig. 11 The relation of % R with cycle number for S/A composite (a) and A (b) samples

Table 4 Comparison between the uptake capacity of the fabricated samples and other adsorbents

Adsorbent	Adsorption capacity (mg/g)	References
Metakaolin based geopolymer	72.300	[34]
EDTA-modified magnetic activated carbon nanocomposite	94.000	[11]
Mo/ Co double layered hydroxide	20.200	[35]
Activated carbon immobilized by tannic acid	1.730	[36]
Crab shell particles	69.900	[37, 38]
Analcime/sodium aluminum silicate hydrate composite	75.188	This study
Analcime	60.241	This study

4 Conclusions

The hydrothermal technique was operated for the construction of sodium aluminum silicate hydrate/analcime composite (abbreviated as S/A) and analcime (abbreviated as A) in the absence and presence of glutamine as phase-controlling template, respectively. The crystallite size of S/A composite and A product is 70.36 and 80.24 nm, respectively. Besides, manganese ions were cost-effectively separated from aqueous solutions utilizing the constructed samples. Moreover, the maximum uptake capacity of S/A composite and A product is 75.188 and 60.241 mg/g, respectively. Furthermore, the constructed products are returnable, stable, effective, and can be reutilized more than once without the concession of their efficacy regarding Mn(II) ions.

Acknowledgements The authors are grateful to the Deanship of Scientific Research, King Saud University for funding through Vice Deanship of Scientific Research Chairs.

Compliance with Ethical Standards

Conflict of interest The authors declare that there is no conflict of interest for this paper.

References

1. M. Visa, Synthesis and characterization of new zeolite materials obtained from fly ash for heavy metals removal in advanced wastewater treatment. *Powder Technol.* **294**, 338–347 (2016)
2. S. Shafiq, A. Nezamzadeh-ejeh, A comprehensive study on the removal of Cd(II) from aqueous solution on a novel pentetic acid-clinoptilolite nanoparticles adsorbent: experimental design, kinetic and thermodynamic aspects. *Solid State Sci.* **99**, 106071 (2020)
3. M. Naushad, G. Sharma, Z.A. Allothman, Photodegradation of toxic dye using Gum Arabic-crosslinked- poly (acrylamide)/Ni(OH)₂/FeOOH nanocomposites hydrogel. *J. Clean. Prod.* **241**, 118263 (2019)
4. Z.N. Garba, I. Lawan, W. Zhou, M. Zhang, L. Wang, Z. Yuan, Microcrystalline cellulose (MCC) based materials as emerging adsorbents for the removal of dyes and heavy metals—a review. *Sci. Total Environ.* **717**, 135070 (2019)
5. E. Nazarzadeh, A. Motahari, M. Sillanpää, Nanoadsorbents based on conducting polymer nanocomposites with main focus on polyaniline and its derivatives for removal of heavy metal ions/dyes: a review. *Environ. Res.* **162**, 173–195 (2018)
6. A. Talaiekhazani, S. Rezaei, Application of photosynthetic bacteria for removal of heavy metals, macro-pollutants and dye from wastewater: a review. *J. Water Process Eng.* **19**, 312–321 (2017)
7. J. Lin, C. Huang, P. Jill, Y. Wang, Fouling mitigation of a dead-end microfiltration by mixing-enhanced preoxidation for Fe and Mn removal from groundwater. *Colloids Surf. A Physicochem. Eng. Asp.* **419**, 87–93 (2013)
8. N. Esfandiari, B. Nasernejad, T. Ebadi, Removal of Mn(II) from groundwater by sugarcane bagasse and activated carbon (a comparative study): application of response surface methodology (RSM). *J. Ind. Eng. Chem.* **20**, 3726–3736 (2014)
9. Y. Zhang, Y. Zhang, X. Zheng, R. Xu, H. He, Grading and quantification of dental fluorosis in zebra fish larva. *Arch. Oral Biol.* **70**, 16–23 (2016)
10. M.R. Lasheen, N.S. Ammar, H.S. Ibrahim, Adsorption/desorption of Cd(II), Cu(II) and Pb(II) using chemically modified orange peel: equilibrium and kinetic studies. *Solid State Sci.* **14**, 202–210 (2012)
11. F. Keyvani, S. Rahpeima, V. Javanbakht, Synthesis of EDTA-modified magnetic activated carbon nanocomposite for removal of permanganate from aqueous solutions. *Solid State Sci.* **83**, 31–42 (2018)
12. Z. Xia, L. Baird, N. Zimmerman, M. Yeager, Heavy metal ion removal by thiol functionalized aluminum oxide hydroxide nanowhiskers. *Appl. Surf. Sci.* **416**, 565–573 (2017)
13. S. Agarwal, I. Tyagi, V. Kumar, M.H. Dehghani, J. Jaafari, D. Balarak, M. Asif, Rapid removal of noxious nickel(II) using novel γ -alumina nanoparticles and multiwalled carbon nanotubes: kinetic and isotherm studies. *J. Mol. Liq.* **224**, 618–623 (2016)
14. W. Zhan, L. Gao, X. Fu, S. Hussain, G. Sui, X. Yang, Green synthesis of amino-functionalized carbon nanotube-graphene hybrid aerogels for high performance heavy metal ions removal. *Appl. Surf. Sci.* **467–468**, 1122–1133 (2019)
15. E.A. Abdelrahman, R.M. Hegazey, Utilization of waste aluminum cans in the fabrication of hydroxysodalite nanoparticles and their chitosan biopolymer composites for the removal of Ni(II) and Pb(II) ions from aqueous solutions: kinetic, equilibrium, and reusability studies. *Microchem. J.* **145**, 18–25 (2019)
16. E.A. Abdelrahman, Synthesis of zeolite nanostructures from waste aluminum cans for efficient removal of malachite green dye from aqueous media. *J. Mol. Liq.* **253**, 72–82 (2018)
17. E.A. Abdelrahman, D.A. Tolan, M.Y. Nassar, A tunable template-assisted hydrothermal synthesis of hydroxysodalite zeolite nanoparticles using various aliphatic organic acids for the removal of Zinc(II) ions from aqueous media. *J. Inorg. Organomet. Polym. Mater.* **29**, 229–247 (2019)
18. E. Erdem, N. Karapinar, R. Donat, The removal of heavy metal cations by natural zeolites. *J. Colloid Interface Sci.* **280**, 309–314 (2004)
19. Y. Taamneh, S. Sharadqah, The removal of heavy metals from aqueous solution using natural Jordanian zeolite. *Appl. Water Sci.* **7**, 2021–2028 (2017)
20. S. Mehdizadeh, S. Sadjadi, S.J. Ahmadi, M. Outokesh, Removal of heavy metals from aqueous solution using platinum nanoparticles/Zeolite-4A. *J. Environ. Heal. Sci. Eng.* **12**, 1–7 (2014)
21. M.G. Lee, G. Yi, B.J. Ahn, F. Roddick, Conversion of coal fly ash into zeolite and heavy metal removal characteristics of the products. *Korean J. Chem. Eng.* **17**, 325–331 (2000)
22. E.A. Abdelrahman, R.M. Hegazey, A. Alharbi, Facile synthesis of mordenite nanoparticles for efficient removal of Pb(II) ions from aqueous media. *J. Inorg. Organomet. Polym. Mater.* (2020). <https://doi.org/10.1007/s10904-019-01238-5>
23. M.Y. Nassar, E.A. Abdelrahman, A.A. Aly, T.Y. Mohamed, A facile synthesis of mordenite zeolite nanostructures for efficient bleaching of crude soybean oil and removal of methylene blue dye from aqueous media. *J. Mol. Liq.* **248**, 302–313 (2017)
24. G. Engelhardt, S. Luger, JCh Buhl, J. Felsche, ²⁹Si MAS n.m.r. of aluminosilicate sodalites: correlations between chemical shifts and structure parameters. *Zeolites* **9**, 1–5 (1989)
25. H.S. Jacobsen, P. Norby, H. Bildsøe, H.J. Jakobsen, 1:1 Correlation between ²⁷Al and ²⁹Si chemical shifts and correlations with lattice structures for some aluminosilicate sodalites. *Zeolites* **9**, 491–495 (1989)
26. R.M. Hegazey, E.A. Abdelrahman, Y.H. Kotp, A.M. Hameed, A. Subaihi, Facile fabrication of hematite nanoparticles from Egyptian insecticide cans for efficient photocatalytic degradation

- of rhodamine B dye. *Integr. Med. Res.* (2020). <https://doi.org/10.1016/j.jmrt.2019.11.090>
27. E.A. Abdelrahman, R.M. Hegazey, R.E. El-Azabawy, Efficient removal of methylene blue dye from aqueous media using Fe/Si, Cr/Si, Ni/Si, and Zn/Si amorphous novel adsorbents. *J. Mater. Res. Technol.* **8**, 5301–5313 (2019)
 28. A. Alharbi, E.A. Abdelrahman, Efficient photocatalytic degradation of malachite green dye using facilely synthesized hematite nanoparticles from Egyptian insecticide cans. *Spectrochim. Acta Part A Mol. Biomol. Spectrosc.* **226**, 117612 (2020)
 29. E.A. Abdelrahman, R.M. Hegazey, Y.H. Kotp, A. Alharbi, Facile synthesis of Fe₂O₃ nanoparticles from Egyptian insecticide cans for efficient photocatalytic degradation of methylene blue and crystal violet dyes. *Spectrochim. Acta Part A Mol. Biomol. Spectrosc.* **222**, 117195 (2019)
 30. E.A. Abdelrahman, R.M. Hegazey, Exploitation of Egyptian insecticide cans in the fabrication of Si/Fe nanostructures and their chitosan polymer composites for the removal of Ni(II), Cu(II), and Zn(II) ions from aqueous solutions. *Compos. Part B* **166**, 382–400 (2019)
 31. M.Y. Nassar, E.A. Abdelrahman, Hydrothermal tuning of the morphology and crystallite size of zeolite nanostructures for simultaneous adsorption and photocatalytic degradation of methylene blue dye. *J. Mol. Liq.* **242**, 364–374 (2017)
 32. E.A. Abdelrahman, A. Subaihi, Application of geopolymers modified with chitosan as novel composites for efficient removal of Hg(II), Cd(II), and Pb(II) ions from aqueous media. *J. Inorg. Organomet. Polym. Mater.* (2019). <https://doi.org/10.1007/s10904-019-01380-0>
 33. M.E. Khalifa, E.A. Abdelrahman, M.M. Hassanien, W.A. Ibrahim, Application of mesoporous silica nanoparticles modified with dibenzoylmethane as a novel composite for efficient removal of Cd(II), Hg(II), and Cu(II) ions from aqueous media. *J. Inorg. Organomet. Polym. Mater.* (2019). <https://doi.org/10.1007/s10904-019-01384-w>
 34. I. Kara, D. Tunc, F. Sayin, S. Tunali, Study on the performance of metakaolin based geopolymer for Mn(II) and Co(II) removal. *Appl. Clay Sci.* **161**, 184–193 (2018)
 35. A.A. Bakr, M.S. Mostafa, E.A. Sultan, Mn(II) removal from aqueous solutions by Co/Mo layered double hydroxide: kinetics and thermodynamics. *Egypt. J. Pet.* **25**, 171–181 (2016)
 36. A. Uyanik, A. Uc, F. Ayg, Adsorption of Cu(II), Cd(II), Zn(II), Mn(II) and Fe(III) ions by tannic acid immobilised activated carbon. *Sep. Purif. Technol.* **47**, 113–118 (2006)
 37. K. Vijayaraghavan, H. Yun, N. Winnie, R. Balasubramanian, Biosorption characteristics of crab shell particles for the removal of manganese(II) and zinc(II) from aqueous solutions. *DES.* **266**, 195–200 (2011)
 38. A. Omri, M. Benzina, Removal of manganese(II) ions from aqueous solutions by adsorption on activated carbon derived a new precursor : Ziziphus spina-christi seeds. *Alexandria Eng. J.* **51**, 343–350 (2012)

Publisher's Note Springer Nature remains neutral with regard to jurisdictional claims in published maps and institutional affiliations.